13th International Conference on CANDU Fuel
Holiday-Inn Waterfront Hotel
Kingston, Ontario, Canada, 2016August 15-18

CANDU FUEL:
Evolution towards Optimal Performance

MULTIPHYSICAL UNSTEADY SIMULATIONS OF BALLOONING PT AND CT CONTACT IN THE BENCHMARK MODEL OF IAEA/ISCP

S.M. Chang[1]and H.T.Kim[2]
[1]Kunsan National University, Gunsan, Jeonbuk, Korea
(558 Daehak-ro, Gunsan, Jeonbuk 54150, Republic of Korea, +82-63-469-4724, smchang@kunsan.ac.kr)
[2]Korea Atomic Energy Research Institute, Daejon, Korea

ABSTRACT – LOCA(loss of coolant accident) is one of the representative severe accident in the operation of nuclear reactors. One of the possible cases is the ballooning of pressure tube and the contact with the Calandria tube for the outer coolant to boil abruptly to saturate. For the moderator system of CANDU-6 reactor, the benchmark model of IAEA/ISCP has been setup to conduct a test and comparison with numerical models on the multi-physics of ballooning PT(pressure tube) and its contact with CT(Calandria tube). The graphite heater is modeled as a volumetric heat source for the given unsteady power of 150 kW, and the PT and CT are installed eccentrically in a given interval. In the first stage, the radiation heat transfer between Zircalloy surfaces of tubes is considered with the same structural deformation model as CATHENA code for the zero-gradient temperature outer boundary condition. A commercial code, COMSOL Multiphysics is used for simulations, and the Gaussian quadrature is applied for the integration of gradient for temperature. The two-dimensional result shows a good agreement for high-order numerical integration in the model with CATHENA one.

Introduction

One of the important design features of a CANDU reactor (a pressurize heavy water reactor) is the use of moderator as a heat sink during some postulated accidents such as a large break Loss Of Coolant Accident (LOCA). If the pressure tube is sufficiently hot while the channel pressure is still relatively high, the pressure tube may radially deform and would fully contact with its surrounding calandria tube (pressure tube/calandria tube ballooning contact). The effectiveness of the moderator heat sink to ensure fuel channel integrity at the onset of this ballooning contact is based on a series of contact boiling experiments [1], which derived the moderator subcooling requirements [2] to preclude a sustained calandria tube dryout by the minimum available moderator subcooling and the pressure tube/calandria tube contact temperature.

International Atomic Energy Agency (IAEA) has launched the International Collaborative Standard Problem (ICSP) to provide a new contact boiling experimental data to assess the subcooling requirements for a heated pressure tube, plastically deforming into contact with the calandria tube during a postulated large break LOCA condition. We participated in 1st Workshop of IAEA ICSP on “HWR Moderator Subcooling Requirements to Demonstrate Backup Heat Sink Capabilities of Moderator during Accidents” (Ottawa, November 2012) [3].

The present study is about preliminary calculation results for these ICSP activity works, where the COMSOL Multiphysics code [4] is used to simulate plastic deformation of a pressure tube as a result of the interaction of stress and temperature. It is shown that the thermal stress model of COMSOL is compatible to simulate the multiple heat transfers (including the radiation heat transfer and heat conduction) and stress strain in the simplified 2 dimensional problem. The benchmark test result for radiation heat transfer is in good agreement with the analytical solution for the concentric configuration of pressure tube and calandria tube. Since the original strain model of COMSOL only considers an elastic deformation with thermal expansion coefficient, the pressure tube/calandria tube contact cannot be predicted in the ICSP problem. Therefore, the plastic deformation model by the Shewfelt and Godin [5], widely used in the CANDU fuel channel analysis, is implemented to the strain equation of COMSOL. The strain rate and the contact time of the pressure tube/calandria tube are calculated for various heating-up conditions of pressure tube to investigate the sensitivity of experimental conditions.

1. Numerical method

In this section, the numerical method and some selected result is presented. The experimental setup [3] and its simplified schematic are given in Fig. 1.

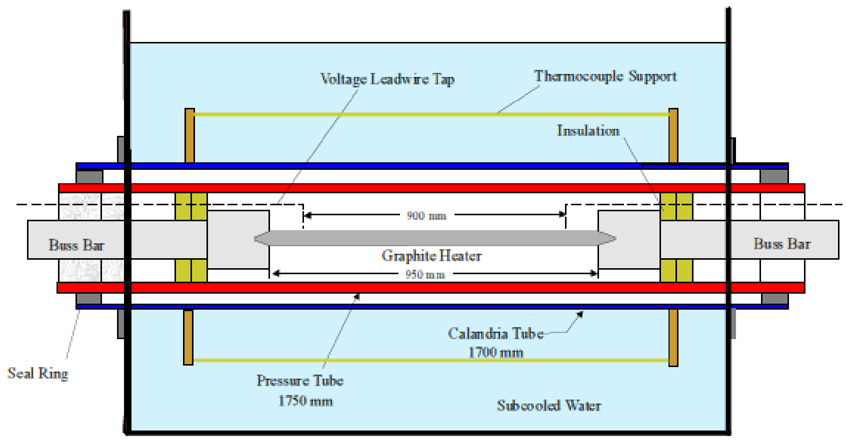

Figure 1 Experimental Setup of IAEA/ICSP Test

The multiphysical simulation is done with the thermal stress(ts) model in the structural mechanics module of a commercial code COMSOL MultyphysicsTM ver. 4.3. The computational domain and boundary condition are given in Fig. 2(a)-(b).
The governing equations are listed as [4]

$$-\nabla \cdot \tilde{\sigma} = \vec{F}_V \tag{1}$$

$$\tilde{\sigma} - \tilde{\sigma}_0 = \tilde{C} : \left[\tilde{\varepsilon} - \tilde{\varepsilon}_0 - \tilde{\alpha}\left(T - T_0\right) \right] \tag{2}$$

$$\frac{\partial \tilde{\varepsilon}}{\partial t} = \frac{1}{2}\left[\left(\nabla \vec{u}\right)^T + \nabla \vec{u} \right] \tag{3}$$

$$\rho C_p \left(\frac{\partial T}{\partial t} + \vec{u} \cdot \nabla T \right) = \nabla \cdot \left(k \nabla T\right) + Q_V \tag{4}$$

Eq. (1) is solved for components of the stress tensor, and the volumetric external force is given as boundary conditions. Note that the stress tensor, later reduced to the plane stress, should be three-dimensional though the computational domain in Fig. 2(a) is 2-D, which is due to the Poisson's ratio in the linear elastic stiffness matrix of Eq. (2). For isotropic materials, the stiffness is expressed as a symmetric square matrix with the six degrees of freedom [6]:

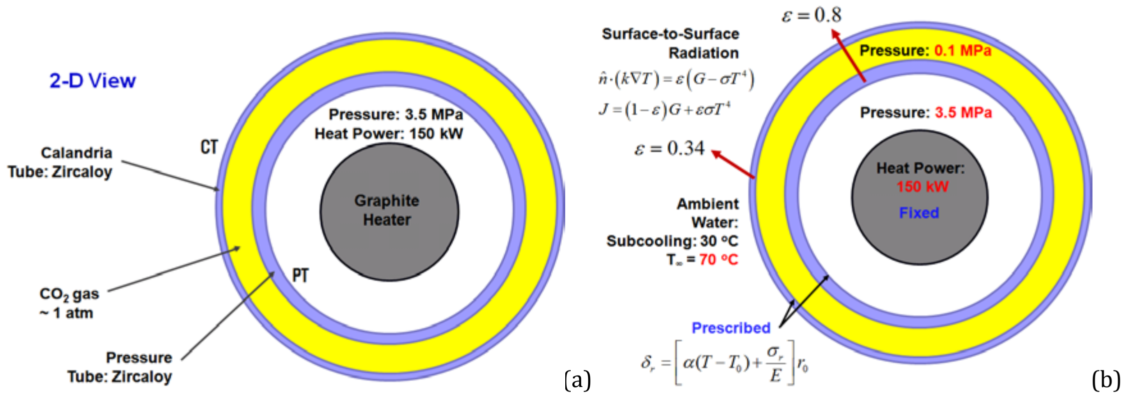

Figure2Computational Conditions:
(a) Computational Domain, (b) Boundary Condition

Structural and thermal strains are coupled in the right hand side of Eq. (2) where the source of temperature is fed back from Eq. (4), the energy equation. From the strain rate, the convective velocity as a function of the global inertia coordinate system is simply obtained from Eq. (3). During each time step, both Eq. (3-4) are integrated by time to calculate a new temperature field for the source term of Eq. (2). The volumetric heat source should be specified inside the field, and other conditions on the temperature and its gradient, or heat flux exerted at all boundaries.

If we assume a very small deformation of initial grids in the global coordinate, Eq. (1-4) are coupled to consist of a complete multi-physical system: structural dynamics and heat transfer. The dominant heat transfer mechanism [3] at the boundaries between the CO_2 gap and each tube is thermal radiation heat transfer, so the others such as convection and conduction will be neglected in this study: the gaseous gap can be deleted from the computational domain in Fig. 2(a), and boundary conditions are marked in Fig. 2(b).

The boundary of core graphite heater is fixed while the inner boundaries of PT and CT should be prescribed as uniform in the radial direction from the thermal expansion and the structural elongation to avoid the numerical instability of asymmetric translation [7]. The load conditions are specified with a constant pressure 3.5 MPa at the core surface and the inner PT, and 0.1 MPa at the outer PT and the inner CT. The emissivity of the core graphite heater, PT, and CT are 1, 0.8, and 0.3, respectively. At the outer boundary of CT, subcooling temperature condition is applied, and the boiling temperature is specified as a constant value of   under the standard atmospheric pressure. Between the core graphite heater and PT as well as PT and CT, a radiation boundary condition is applied.

The material of PT and CT is Zircaloy 2 that is a kind of Zirconium alloy. The specific heat capacity and the heat conductivity [9, 10] are functions of temperature, andstructural correlations are obtained from the fitting of experimental data in the similar way [11, 12]. Fig. 3 shows the computational grids for the present problem.

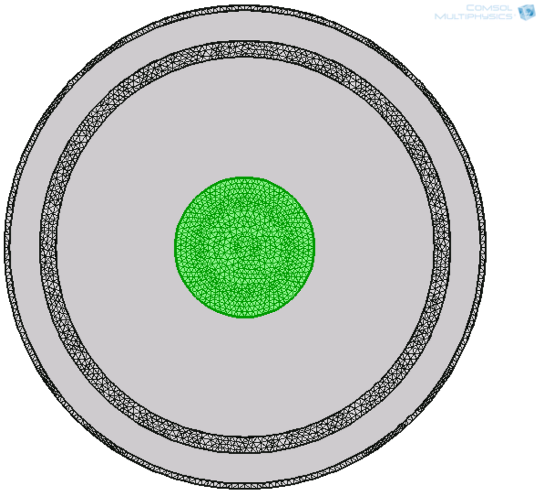

Figure3Computational Grids

2. Numerical model

During abnormal accident conditions such as a large LOCA without emergency core cooling in CANDU6 reactors, the PT is overheated and may undergo plastic deformation and growth. Plastic deformation is a permanent dimensional change, which occurs as a result of the interaction of stress and temperature. This deformation is known as PT ballooning or creep. The strain model in Equations (5) is from the model of linear elasticity. The structural behavior over the yield strength of material should be considered in the high temperature region.

The creeping model [5] for the CATHENA code is also used in the present research. The linear elastic model should be substituted to follow

$$\dot{\varepsilon} = \frac{d\varepsilon}{dt} = \begin{cases} \left(1.3\times10^{-5}\right)\sigma^{9}e^{-36600/T} + \dfrac{\left(5.7\times10^{7}\right)\sigma^{1.8}e^{-29200/T}}{\left[1+\left(2\times10^{10}\right)\int_{t_1}^{t} e^{-29200/T}dt\right]^{0.42}}, & 973K \le T \le 1123K \\ \left(10.4\right)\sigma^{3.4}e^{-19600/T} + \dfrac{\left(3.5\times10^{4}\right)\sigma^{1.4}e^{-19600/T}}{1+\left(274\right)\int_{t_2}^{t} e^{-19600/T}\left(T-1105\right)^{3.72}dt}, & 1123K \le T \le 1473K \end{cases} \tag{5}$$

where , and and are times at temperature and , respectively.

Unfortunately, the time integration at the denominator of Eq. (5) cannot be expressed in the analytic form, which needs some approximation. Using the two-point Gaussian quadrature for these integrations [13].

This appoxiamtion is also applied to the integration for the displacement as follows:

$$\delta_r = \left[\int_{T_0}^{T} \alpha dT + \frac{\sigma_r}{E}\right] r_0 \tag{6}$$

2.1 Two-point Gaussian quadrature approximation

The strain rate in Equation (5) is expressed in an explicit form:

$$\dot{\varepsilon}=\begin{cases}\left(4.99\times10^{9}\right)e^{-36600/T}+\dfrac{\left(4.71\times10^{10}\right)e^{-29200/T}}{\left[1+\left(3.01\times10^{8}\right)\left(T-973\right)\left(e^{\frac{-29200}{0.7887T+206}}+e^{\frac{-29200}{0.2113T+767}}\right)\right]^{0.42}}, & 973K\le T\le 1123K\\ \left(3.36\times10^{6}\right)e^{-19600/T}+\dfrac{\left(6.50\times10^{6}\right)e^{-19600/T}}{1+\left(4.12\right)\left(T-1123\right)\left[\begin{array}{l}e^{\frac{-19600}{0.7887T+237}}\left(0.7887T-868\right)^{3.72}\\ +e^{\frac{-19600}{0.2113T+886}}\left(0.2113T-219\right)^{3.72}\end{array}\right]}, & 1123K\le T\le 1473K\end{cases} \tag{7}$$

2.2 Four-point Gaussian quadrature approximation

The more precise approxiation for Equation (5) is extended to

$$\dot{\varepsilon}=\begin{cases}(4.99\times10^{9})e^{-\frac{36600}{T}}+\dfrac{(4.71\times10^{10})e^{-\frac{29200}{T}}}{\left[1+(1\times10^{10})\dfrac{(T-T_1)}{\dot{T}}\left\{\begin{array}{l}0.3479\left(\begin{array}{l}e^{\frac{-29200}{0.06943T+0.9306T_1}}\\ +e^{\frac{-29200}{0.06943T_1+0.9306T}}\end{array}\right)\\ +0.6521\left(\begin{array}{l}e^{\frac{-29200}{0.33T+0.67T_1}}\\ +e^{\frac{-29200}{0.33T_1+0.67T}}\end{array}\right)\end{array}\right\}\right]^{0.42}}, & 773K\le T\le 1123K;\\ (3.36\times10^{6})e^{-\frac{19600}{T}}+\dfrac{(6.50\times10^{6})e^{-\frac{19600}{T}}}{1+(137)\dfrac{(T-T_2)}{\dot{T}}\left[\begin{array}{l}0.3479\left\{\begin{array}{l}e^{\frac{-19600}{0.06943T+0.9306T_2}}\left(0.06943T+0.9306T_2-1105\right)^{3.72}\\ +e^{\frac{-19600}{0.06943T_2+0.9306T}}\left(0.06943T_2+0.9306T-1105\right)^{3.72}\end{array}\right\}\\ +0.6521\left\{\begin{array}{l}e^{\frac{-19600}{0.33T+0.67T_2}}\left(0.33T+0.67T_2-1105\right)^{3.72}\\ +e^{\frac{-19600}{0.33T_2+0.67T}}\left(0.33T_2+0.67T-1105\right)^{3.72}\end{array}\right\}\end{array}\right]}, & 1123K\le T\le 1473K;\end{cases} \tag{8}$$

The difference of Equations (7-8) is compared in Fig. 4 for the expansion ratio of the structure. The higher order model shows a sharp discontinuity from in the deformation model of Shewfelt and Godin. As the 2-point Gaussian quadrature slightly under-estimates the expansion ratio less than four-point approximation before the contact, or the contact time is over-estimated in 3.75% error. However, in the two-point approximation over-estimates more than high-order numerical method reversely, and therefore the slightly less slope of and of COMSOL results in Figures 5 and 6 can be explained naturally.

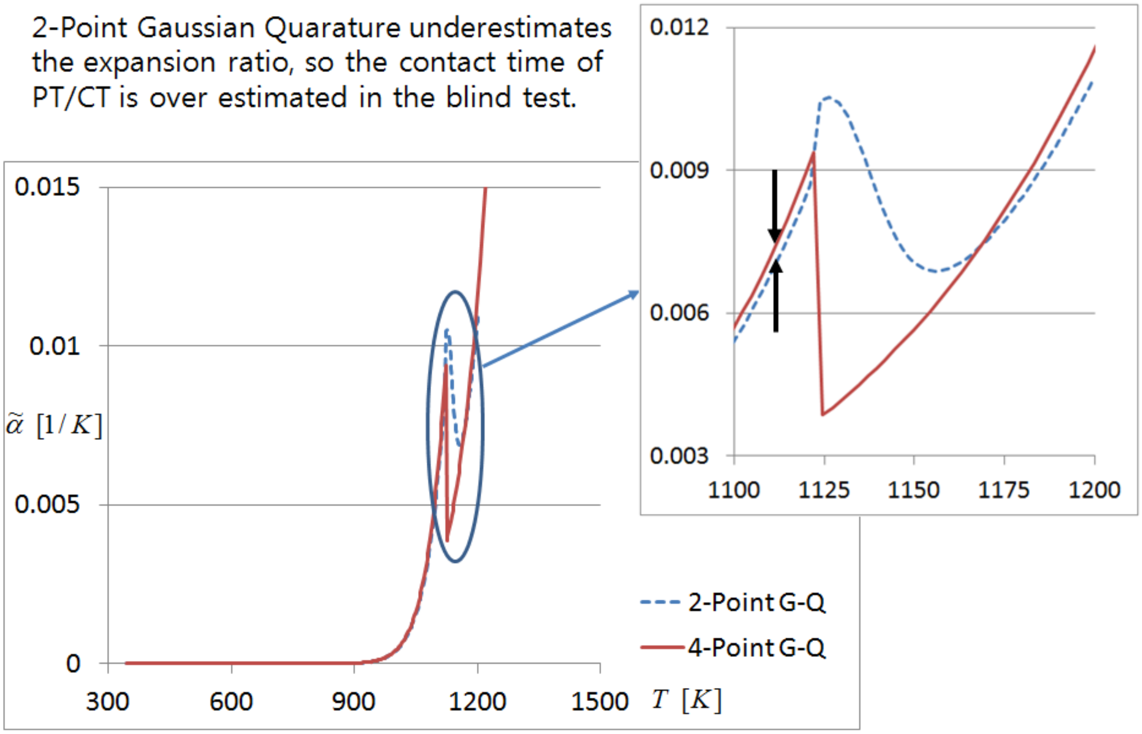

Figure4Comparison of Gasussian Quadrature Models

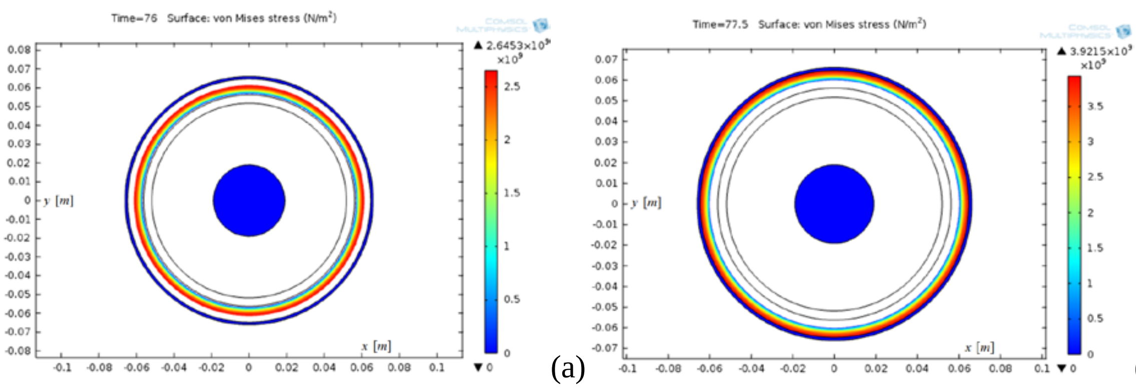

(a) (b)

Figure5Prediction of Pressure Tube Contact:
(a) Before Contact, (b) After Contact

3. Result and discussion

The COMSOL Multiphysics solver integrates Equations (1-4) with FEM (finite element method) schemes, and the approximate solution is obtained by time marching. The heat source in Eq. (4) is given by heater power boundary condition (BC) as shown in Fig, 2(b). The constant temperature boundary condition (70˚C) is given to outside surface of CT in the first stage before contact, but the heat flux is fixed zero, or adiabatic in the later stage after contact where the outer boundary condition on CT should be modified with convection and boiling models. In the present step, the adiabatic outer BC is just imposed to compare with the result from CATHENA code.

Figure 5(a-b) shows the results of von Mises stress and configuration of PT expansion before/after contact time. The PT is ballooned to contact with CT at 77.5 second. The PT at time of 76 second (Figure 5(a)) starts to expand and rapidly contact with CT within 1.5 second (Figure 5(b)). The present computation uses the 3rd order, or two-point Gaussian quadrature for the numerical integrations.

Under the same condition as CATHANA code [9], the simulation is done, and the final result for temperature and strain in Figures 6 and 7, respectively. CATHENA code results are compared with those of the COMSOL code. The PT/CT contact time by CATHENA calculation is 71.5 second, which is earlier than that by the COMSOL prediction. However the heat-up of PT and strain results are in good qualitative agreement at least as shown in Figures 6 and 7, respectively.

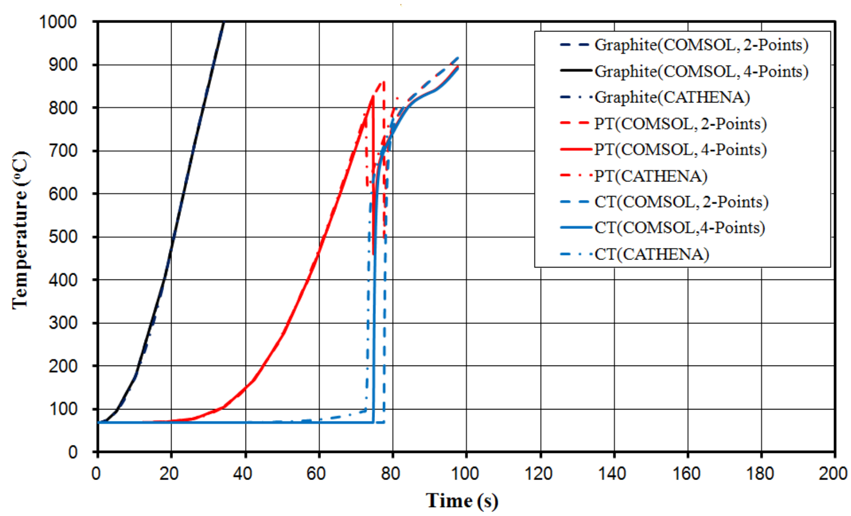

Figure 6 Comparison of Outside Wall Temperature Predictions

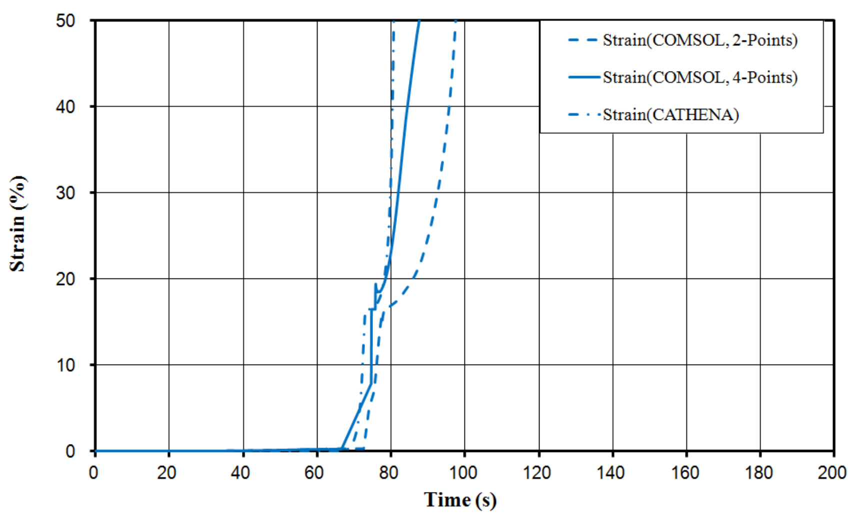

Figure 7 Comparison of Tube StrainPredictions

The quantitative inconsistency of the contact time is due to the numerical error for the rapidly varying grids in the integration of Eq. (5). If we select more points of Gaussian quadrature such as Equation (8), the contact time can be reduced to 74.6 seconds (7th order, or four points), for example. The higher order numerical method shows that the curves in Figures 6 and 7 are closer to the result of CATHENA code.

4. Conclusions

Unsteady two-dimensional multi-physical simulation has been numerically setup with the thermal stress module in COMSOL Multiphysics. The core heater, PT, and CT are modeled from the geometry configuration of the test apparatus simulating the horizontal fuel channel of a CANDU type reactor. To avoid other installation effects, the configuration of tubes is arranged concentric, and the inner boundaries are prescribed to satisfy the radial symmetry. The radiation surface-to-surface boundary condition between tubes is validated to have a very small error only in 0.6% for this numerical computation from the classical analytic solution.

The results of numerical simulation in the present work are shown that:

(1) With linear thermal elastic model, the expansion of PT is very small, and the solution converges to the steady state within hundreds seconds. This result implies that the only component that makes the computation unstable is the plastic thermal deformation of tubes.

(2) When the present computational model is extended with a plastic deformation model, the sudden radial expansion or ballooning is globally observed in the system of concentric tube. PT expands within several milliseconds at 77 second from the initial condition to contact with outer CT. The temperature between the heated PT and CT undergoing the subcooling environment is high temperature of about 760 K, and the union of PT and CT will be faced to a great heat sink after the contact.

(3)With the higher order accuracy for the numerical method of Gaussian quadrature from 3rd (2-point) to 7th(4-point), the CT/PT contact time is reduced about 3 seconds, and the slopes of temperature and strain were a little reduced after contact, which should be considered as more realistic one.

5. References

[1] G.E. Gillespie, "An Experimental Investigation of Heat Transfer from a Reactor Fuel Channel: To Surrounding Water," Proceedings of 2nd Annual Conference of the Canadian Nuclear Society, Ottawa, Canada, 1981.

[2] H.Z. Fan, R. Aboud, P. Neal and T. Nitheanandan, "Enhancement of the Moderator Subcooling Margin using Glass-peened Calandria Tubes in CANDU Reactors," Proceedings of 30th Annual Conference of the Canadian Nuclear Society, Calgary, Canada, 2009.

[3] T. Nitheanandan, “Proposal for the IAEA International Collaborative Standard Problem on HWR Moderator Subcooling Requirements to Demonstrate Backup Heat Sink Capabilities of Moderator during Accidents,” http://www.iaea.org/NuclearPower/WCR/ICSP-HWR-Moderator.html, 2012.

[4] COMSOL Multiphysics, “Structural Mechanics User's Guide,” Theory for the Solid Mechanics Interface, ver. 4.4, 2012, pp. 160-170.

[5] R.S.W. Shewfelt, L. Lyall, D.P. Godin, “A High-Temperature Creep Model for Zr-2.5%Nb Pressure Tubes,” Journal of Nuclear Materials, No. 125. also found in Strain Model of CATHENA Code, 2012, 153-112020-STM-001, 1984, pp. 5-25.
.
[6] T.H.G. Megson, Aircraft Structures for Engineering Students, Edward Arnolds, Bristol, England, 1985, pp. 22-25.

[7] S.M. Chang, H.T. Kim, “Unsteady Two-Dimensional Multiphysical Simulation on the Radiating Calandria Tube Under the Subcooling Boundary Condition,” Transaction of Korean Nuclear Society, Autumn Meeting, 2012October 25-26.

[8] Y. Cengel, Introduction to Thermodynamics and Heat Transfer: Vol. II Heat Transfer, International Editions, McGraw-Hill Higher Education, 2001, pp. 670.

[9] T.G. Beuthe, B.N. Hanna (editors), “CATHENA MOD-3.5c/Rev 0 Theoretical Manual,” CANDU Owners Group Report, COG-99-007, 1999.

[10] MATPRO-Ver. 11 (Rev. 1), a handbook of material properties for use in the analysis of light water reactor fuel rod behavior, NUREG/CR-0497, TREE-1280, 1980.

[11] K. J. Geelhood, C. E. Beyer, and W. G. Luscher, “PNNL Stress/Strain Correlation for Zircaloy,” Pacific Northwest National Laboratory, PNNL-17700, 2008.

[12] W. G. Luscher, K. J. Geelhood, “Material Property Correlations: Comparisons between FRAPCON-3.4, FRAPTRAN 1.4, and MATPRO,” (NUREG/CR-7024) PNNL-19417, NRC, United States, 2011.

[13] S. C. Chapra and R. P. Canale, Numerical Methods for Engineers, 2nd edition, McGraw-Hill International, 1988, pp. 511-519.